

Scalar Isoscalar pion pairs in nuclei and the $A(\pi, \pi\pi)X$ reaction

M.J. Vicente Vacas and E. Oset

Departamento de Física Teórica and IFIC, Centro Mixto Universidad de Valencia-CSIC,

46100 Burjassot, Valencia, Spain

(September 17, 2018)

Abstract

The reaction $A(\pi, \pi\pi)X$ has been studied at low energies, paying particular attention to the interaction of the two final pions in the scalar isoscalar ($I=J=0$) channel. We have developed a microscopic model for the pion production, and then implemented the two pion final state interaction by using the results of a non-perturbative unitary coupled-channels method based in the standard chiral Lagrangians. The resulting model, describes well the reaction on the nucleon for all different isospin channels. Finally, we have considered the reaction in nuclei. Our calculation takes into account Fermi motion, Pauli blocking, pion absorption, and also the strong modification of the $\pi\pi$ interaction in the nuclear medium.

13.60.Le,13.75.Lb,13.75.Gx,21.65+f,25.80.Hp

I. INTRODUCTION

The reaction $A(\pi, \pi\pi)X$ has attracted much interest lately, as a means to investigate the properties of correlated $I = J = 0$ pion pairs, the " σ " meson, in nuclear matter [1,2]. This has been partly motivated by recent experimental results, which show an A dependent large enhancement of the cross section at low invariant masses of the dipion system [3,4]. The enhancement occurs for the $A(\pi^-, \pi^+\pi^-)X$ process ($I_{\pi\pi} = 0$ and 2 at low energies), but is conspicuously absent for the $A(\pi^+, \pi^+\pi^+)X$ case ($I_{\pi\pi} = 2$). Thus, it happens only when $I_{\pi\pi} = 0$ pion pairs are produced, and could be related to the medium dependence of the $\pi\pi$ interaction in the σ channel.

Our theoretical understanding of the $\pi\pi$ scattering in vacuum has improved considerably in the last few years. Close to threshold, the $\pi\pi$ interaction is well described by Chiral Perturbation Theory (χ PT). At higher energies, where unitarity matters and we are out of the χ PT range of validity, some very successful non perturbative models have been developed [5,6]. They are able to give a good description of the $\pi\pi$ scattering in the σ channel up to energies above 1 GeV.

Whereas in vacuum the low energy $\pi\pi$ interaction in the $I = J = 0$ channel, although attractive, is too weak to admit a bound state, it was soon realized that the nuclear medium attraction of the pions could lead to the accumulation of some strength close to the two pion threshold, or even to the appearance of a new bound state [7]. A similar conclusion has been reached in Ref. [2], where an enhancement of the the spectral function in the σ channel, just above the 2π threshold, has been predicted as a consequence of a possible partial restoration of chiral symmetry in the nuclear medium. Actually, in more detailed calculations, based on the $\pi\pi$ interaction model of ref. [5] it has been found that spontaneous s-wave pion pair condensation could appear at densities as low as ρ_0 [8–10]. Further works along the same line, but using the chirally improved Jülich model for the meson-meson interaction, have shown that instabilities are pushed up in density when chiral constraints are imposed [11,12]. Nonetheless, some accumulation of strength close to the two pion

threshold was found. Similar results have been obtained in ref. [13]. The latter work is based in the model for $\pi\pi$ interaction of ref. [6], which generates the scattering amplitude using the chiral lagrangians, and then unitarizes it by the inverse amplitude method.

The first experimental signals showing a small enhancement of the $\pi\pi$ spectral function in the $A(\pi, 2\pi)X$ reaction were found in ref. [14], although the experiment didn't measure below $M_{\pi\pi} = 300$ MeV, and hence, missed the most interesting region. The advent of CHAOS improved considerably the experimental possibilities, and it has provided us with a wealth of good quality data for several charge channels and nuclei. The results show the emergence of a very clear peak in the $M_{\pi\pi}$ spectral function close to threshold, when pions in the scalar isoscalar channels are present in the final state [3,4,15]. This peak, absent for the reaction on deuterium already appears on light nuclei, and grows as a function of the atomic number. In contrast, only minor changes are observed when the cross section of the $(\pi^+, 2\pi^+)$ reaction in deuterium is compared to the same process in heavier nuclei. Certainly, the different behaviour of the two processes cannot be caused by trivial nuclear effects, like Fermi motion, Pauli blocking, or pion absorption, which are practically identical for both cases.

In ref. [1], a calculation of the $A(\pi, 2\pi)X$ reaction has been presented in which the $\pi\pi$ FSI was taken into account using the approach of ref. [11]. The emphasis being placed on the analysis of FSI, the elementary mechanism of pion production on a single nucleon ($\pi N \rightarrow \pi\pi N$) was described in a simplified manner, taking only the most important pieces of the amplitude. Also, some simplifications were done on the treatment of nuclear effects, like Fermi motion, or pion absorption. The results are very stimulating, and show some enhancement on the $M_{\pi\pi}$ distribution close to threshold, which agrees well with the experimental data.

Our aim in this paper is to do a more detailed study of the reaction, including a realistic $\pi N \rightarrow \pi\pi N$ amplitude, and incorporating some nuclear effects omitted in the previous work, and which could affect its conclusions.

In sec. II we give a brief outline of the model for $\pi\pi$ scattering in the scalar isoscalar

channel both in vacuum [6] and in nuclear matter [13]. Then, in sec. III we develop a model for the $\pi N \rightarrow \pi\pi N$ reaction. Finally, in sec. IV we discuss the process in nuclei.

II. BASIC THEORY OF THE $\pi\pi$ SCATTERING IN THE SCALAR ISOSCALAR CHANNEL

A. $\pi\pi$ scattering in vacuum

The $\pi\pi$ scattering amplitude is calculated solving the coupled channels Bethe-Salpeter (BS) equation

$$T_{\pi\pi} = \mathcal{V}_{\pi\pi} + \mathcal{V}_{\pi l} \mathcal{G}_{ll} T_{l\pi}, \quad (1)$$

where the subindex π corresponds to the state $|\pi\pi, I = 0\rangle$ and the subindex l accounts for the $|\pi\pi, I = 0\rangle$ and the $|K\bar{K}, I = 0\rangle$ states. The potentials \mathcal{V}_{ij} are obtained from the lowest order chiral Lagrangians [16]. Explicit expressions can be found in Ref. [13]. The $\mathcal{V}\mathcal{G}T$ term of eq. 1 stands for

$$\mathcal{V}\mathcal{G}T = \int \frac{d^4k}{(2\pi)^4} \mathcal{V}(q_1, q_2, k) \mathcal{G}(P, k) T(k; q'_1, q'_2), \quad (2)$$

where q, q', P , and k are the momenta of the mesons as defined in fig. 1. A cutoff ($q_{max} = 1$ GeV) is used in the evaluation of the integral. $\mathcal{G}(P, k)$ is the product of the two meson propagators in the loop,

$$\mathcal{G}_{lj}(P, k) = i \frac{1}{k^2 - m_l^2 + i\epsilon} \frac{1}{(P - k)^2 - m_j^2 + i\epsilon}. \quad (3)$$

The particular \mathcal{V}_{ij} off-shell dependence leads to the simplification of the integral BS equation which can be transformed into the purely algebraic expression

$$T_{ik} = V_{ik} + V_{ij} G_{jj} T_{jk}, \quad (4)$$

where V_{il} is now the on-shell part of the potentials (when the momenta are taken such that $p_i^2 = m_i^2$), and

$$G_{jj} = i \int \frac{d^4k}{(2\pi)^4} \frac{1}{k^2 - m_{1j}^2 + i\epsilon} \frac{1}{(P-k)^2 - m_{2j}^2 + i\epsilon}. \quad (5)$$

The resulting amplitude reproduces well experimental phase shifts and inelasticities in the $I = J = 0$ channel up to 1.2 GeV.

B. $\pi\pi$ in nuclear matter

In the nuclear medium, the pion propagators are strongly modified, mainly due to their coupling to particle-hole (ph) and Δ -hole (Δh) excitations. Therefore, new terms, of the type depicted in fig. 2 have to be included in the calculation of the scattering amplitude. It has been shown [17,13] that the terms c),d),f),... of fig. 2 cancel the off shell contribution of the terms a),b),e),... so that only these latter terms must be considered with the $\pi\pi$ amplitudes factorized on shell. As a result the new BS equation is written as

$$T_{\pi\pi} = V_{\pi\pi} + V_{\pi K} G_{KK} T_{K\pi} + V_{\pi\pi} \tilde{G}_{\pi\pi} T_{\pi\pi}. \quad (6)$$

As the $K\bar{K}$ state contributes very little to $T_{\pi\pi}$ at low energies, the vacuum values are kept for G_{KK} . Only $T_{\pi\pi}$ and $\tilde{G}_{\pi\pi}$ are renormalized in the medium. The function $\tilde{G}_{\pi\pi}$ is now given by

$$\tilde{G}_{\pi\pi} = i \int \frac{d^4k}{(2\pi)^4} \frac{1}{k^2 - m_\pi^2 - \Pi(k)} \frac{1}{(P-k)^2 - m_j^2 - \Pi(P-k)}, \quad (7)$$

where $\Pi(k)$ is the pion selfenergy in the nuclear medium calculated as

$$\Pi(k) = \frac{(\frac{f}{m_\pi})^2 \vec{k}^2 U(k)}{1 - (\frac{f}{m_\pi})^2 g' U(k)}, \quad (8)$$

with g' the Landau-Migdal parameter ($g' = 0.7$), f the $NN\pi$ coupling constant ($f = 1$), and U the Lindhard function for both ph and Δh excitations [18]. In addition, we have also included the contribution of $2p2h$ excitations as explained in ref. [13].

In fig. 3 we show the imaginary part of the $\pi\pi$ scattering amplitude for several nuclear densities. The results show a displacement of strength towards low energies. Although eq. 6 leads to a zero value for the amplitude close to the Adler's zero, ($s = m_\pi^2/2$ with s

the Mandelstam variable of the two pions system), the accumulation of strength close and below the two pion threshold is large and grows rapidly as a function of the nuclear density. Very similar results were found in other works using different models for $\pi\pi$ interaction but imposing some minimal chiral constraints. See, for instance, fig. 12 of ref. [12] and fig. 3 of ref. [19].

III. THE $\pi N \rightarrow \pi\pi N$ REACTION

Our understanding of the $\pi N \rightarrow \pi\pi N$ reaction at low energies has improved considerably in the last few years both experimentally and theoretically [20–24]. The model we present here follows closely that of ref. [20], where only the $\pi^- p \rightarrow \pi^+ \pi^- n$ process was calculated. In this paper we will extend it to other charge channels and will include additional mechanisms, that have been found to be important in the calculation of some differential cross sections [25,4].

At low energies, the only particles that need to be considered are pions, nucleons, and the Δ and Roper resonances. The need of the latter seems surprising, because of its relatively high mass and the smallness of the πNN^* coupling. However, the Roper resonance partly decays to a nucleon and a s-wave pion pair. This mechanism does not vanish at threshold, unlike most other terms, and it has been found to be very important for all charge channels that allow for an $I=J=0$ pion pair [25].

We have considered in our model the mechanisms represented by the diagrams of fig. 4. The dashed lines are pions, and the internal solid lines are all possible baryons (N, N^*, Δ). Notice, that different charge channels allow or forbid some of the diagrams. Also all possible different time orderings, not explicitly depicted, are included in the actual calculation. The Feynman rules used to calculate the scattering amplitude are derived from the effective Lagrangians of the Appendix. It is relevant to mention here that no attempt to fit the $\pi N \rightarrow \pi\pi N$ data has been made. Rather, standard values for the coupling constants, obtained from different experiments and/or analysis, have been used.

A. Isospin amplitudes

The scattering amplitudes for the different $\pi N \rightarrow \pi\pi N$ charge channels can be written as linear combinations of four isospin amplitudes $T_{2I, I_{\pi, \pi}}$. Here, I and $I_{\pi, \pi}$ are the total isospin of the system and the isospin of the two final pions. The expressions, for the channels we are interested in, are

$$T(\pi^- p \rightarrow \pi^+ \pi^- n) = -\frac{1}{\sqrt{45}}T_{32} + \frac{\sqrt{2}}{3}T_{10} + \frac{1}{3}(T_{11} - T_{31}), \quad (9)$$

$$T(\pi^- p \rightarrow \pi^0 \pi^0 n) = \frac{4}{\sqrt{45}}T_{32} + \frac{\sqrt{2}}{3}T_{10}, \quad (10)$$

$$T(\pi^+ p \rightarrow \pi^+ \pi^+ n) = -\frac{2}{\sqrt{5}}T_{32}. \quad (11)$$

Before proceeding, it is interesting to make some qualitative considerations. The symmetry of the pion pair wave function implies that the orbital angular momentum of the two final state pions will be even for the T_{10}, T_{32} and odd for the $I_{\pi\pi} = 1$ amplitudes. Thus, at low enough energies, where only s-wave would dominate, both T_{11} and T_{31} should be negligible. On the other hand, the cross section for the $\pi^+ p \rightarrow \pi^+ \pi^+ n$ channel is much smaller than for the other two cases. Therefore $T_{32} < T_{10}$, what implies that the amplitudes for the $\pi^+ \pi^-$ and for the $\pi^0 \pi^0$ case should be equal at low energies and also that they are, essentially, dominated by the production of scalar isoscalar pion pairs. As a consequence, the $\pi^0 \pi^0$ cross section should be about one half the one for $\pi^+ \pi^-$, once the different thresholds are taken into account. Of course, the energies at which there are experimental data are not that close to threshold and one cannot neglect T_{11} and T_{31} . In our calculation, we will proceed as follows. First, using the Lagrangians of the appendix we calculate the amplitudes for the different charge channels. Then, by means of eqs. 9, 10 and 11, we obtain T_{10}, T_{32} , and the combination $T_{11} - T_{31}$, and finally, we modify T_{10} by including the final state interaction of the $I = J = 0$ pion pairs .

At low energies, due to the smallness of the $I_{\pi\pi} = 1$ contributions, we only need to consider the effects of the FSI on the $I_{\pi\pi} = 0, 2$ channels. Furthermore, as it is shown in ref.

[1] the $\pi\pi$ interaction in for $I_{\pi\pi} = 2$ is quite weak and does not change appreciably inside the nuclear medium. Thus only the FSI on the $I_{\pi\pi} = 0$ channel could produce large effects on the scattering amplitude both in vacuum and in nuclei. To account for it, the amplitude T_{10} is modified in the following manner,

$$\tilde{T}_{10} = T_{10}\mathcal{F} = T_{10} + T_{10}\tilde{G}_{\pi\pi}T_{\pi\pi} \quad (12)$$

where $\tilde{G}_{\pi\pi}$ and $T_{\pi\pi}$ are the two pions propagator and the scalar isoscalar two pions amplitude defined in eqs. 7 and 6 respectively. Using again eqs. 9, 10 and 11, where T_{10} is now replaced by \tilde{T}_{10} we obtain the scattering amplitudes for the physical channels.

As can be seen in fig. 5, this model, without free parameters, reproduces fairly well the total cross sections for the three channels considered. This agreement extends to differential cross sections, as it will be shown for some cases in next section. The net effect of the inclusion of the pions FSI is a small enhancement of the total cross section for the $\pi^+\pi^-$ and $\pi^0\pi^0$ channels, and slight modifications of the differential cross sections, as it was expected, given that the \mathcal{F} factor changes very smoothly, in vacuum, over the available phase space.

IV. THE $\pi A \rightarrow \pi\pi X$ REACTION

There are several nuclear effects that could modify the pion production cross section, like Fermi motion, Pauli blocking, pion absorption and quasielastic scattering. Additionally, there could be new reaction mechanisms involving more than one nucleon, but the contribution of this kind of processes has been shown to be quite small [4]. To account for the medium effects we follow ref. [33]. Assuming only one nucleon mechanisms, the cross section can be written as

$$\sigma = \frac{\pi}{q} \int d^2\vec{b} dz F_{ISI} \int \frac{d^3\vec{k}}{(2\pi)^3} \int \frac{d^3\vec{q}_1}{(2\pi)^3} \int \frac{d^3\vec{q}_2}{(2\pi)^3} n(|\vec{k}|) (1 - n(|\vec{q} + \vec{k} - \vec{q}_1 - \vec{q}_2|)) \quad (13)$$

$$\sum_{s_i s_f} |T|^2 \frac{1}{2\omega(\vec{q}_1)} \frac{1}{2\omega(\vec{q}_2)} \delta(q^0 + E(\vec{k}) - \omega(\vec{q}_1) - \omega(\vec{q}_2) - E(\vec{q} + \vec{k} - \vec{q}_1 - \vec{q}_2)) F_{out-abs}, \quad (14)$$

where $\vec{q}, \vec{k}, \vec{q}_1$, and \vec{q}_2 are the initial pion, initial nucleon and two final pions momenta; $E(\vec{k}), \omega(\vec{q}_1)$ and $\omega(\vec{q}_2)$ are their energies. The spatial volume element is written in terms

of \vec{b} , perpendicular, and z parallel to the beam momentum. The occupation number $n(\cdot)$ refers to the local density, it takes the value 1 when the argument is below the local Fermi momentum ($k_F = (3\pi^2\rho(\vec{b}, z)/2)$) and zero above it. Note the sum over initial and final spins, but not over isospin because the channels we study involve only protons in the initial state and neutrons in the final one. In this paper, we only consider symmetric nuclei, and we will use the same density for neutrons and protons. The nuclear densities are taken from ref. [34]. The amplitude T is also evaluated at the local density, what fundamentally means that its only changes occur in the \mathcal{F} factor, related to the $\pi\pi$ interaction. Finally, the factors F_{ISI} , and F_{out_abs} account for the flux loss due to pion absorption and scattering in the case of F_{ISI} and for pion absorption alone in the case of F_{out_abs} . Both pion absorption and quasielastic scattering are quite strong at the energy of the incoming pion and both reduce the effective initial pion flux. That is clear for the absorption, but it is also true for the π -nucleus quasielastic scattering, because in these collisions the pion loses always some energy, what reduces enormously the possibility of a subsequent pion production. We implement the flux lost with the eikonal factor

$$F_{ISI} = \exp\left(\int_{-\infty}^z dz' (P_{abs}(\omega(q), \rho) + P_{qua}(\omega(q), \rho))\right), \quad (15)$$

where P_{abs}, P_{qua} are the absorption and quasielastic scattering probability per unit length, that we take from ref. [33]. Due to these interactions, the flux reaching the inner nucleus is quite small and the reaction happens at the surface, what reduces considerably the possibility of strong medium effects. As mentioned in ref. [1], the final pions have low energy and absorption or quasielastic scattering is a minor effect in their case. This has also been confirmed in the analysis of experimental data of ref. [14]. Nonetheless, it could affect more those events happening at high densities in the center of the nucleus. Therefore, we include the factor F_{out_abs} that calculates the reduction of the cross section due to the absorption of any of the final pions. It is given by

$$F_{out_abs} = \exp\left(\int_{-\vec{b}, z}^{\infty} dl_1 P_{abs}(\omega(q_1), \rho)\right) \exp\left(\int_{-\vec{b}, z}^{\infty} dl_2 P_{abs}(\omega(q_2), \rho)\right), \quad (16)$$

where dl_1 , dl_2 are the elements of longitude along the \vec{q}_1 and \vec{q}_2 directions. The probability of quasielastic collisions is very small at these energies and we ignore it.

V. RESULTS

The results that will be presented in this section are all compared with CHAOS data. We have approximately implemented the experimental acceptance cuts in our calculation. Let us take the beam direction as the z -axis, and x forming with z the horizontal plane, then $\phi = 0 \pm 7$ degrees, where ϕ is the pion angle with the xz plane, and $10 < \theta < 170$, with θ the pion angle with the z direction. Also, we have taken a pion kinetic energy threshold, $T_\pi > 11 \text{ MeV}$.

In fig. 6, we show the invariant mass distributions for the deuteron case. We obtain a quite good agreement in the $\pi^+\pi^+$ channel in both shape and size. The agreement is not as satisfactory for the $\pi^+\pi^-$ case. As can be seen in fig. 5, the total cross section is slightly overestimated by our model, and a similar situation is found for the mass distribution. In order to compare easily with the experimental shape, we have renormalized our result reducing it by a 20% and this is what is shown in the figure. Let us remember here, that no parameter has been adjusted, and some of them, like those related to the Roper properties are very uncertain. A quite small change of a few percent in the Roper coupling constants would produce a fine agreement in size. It is interesting to understand the quite different behaviour of the two channels under consideration. As it was already stressed in ref. [4], the $\pi^+\pi^+$ case follows closely a pure phase space distribution. The two peaks of the figure respond only to the geometry of the experimental apparatus, which favours clearly the situations in which either the pions go together (low $M_{\pi\pi}$) or in opposite directions (high $M_{\pi\pi}$). The smallness of the $M_{\pi\pi}$ distribution in the $\pi^+\pi^-$ reaction reflects the much richer structure of the amplitude, and it is produced by the destructive interference of large pieces. Consider, as an example, the mechanisms (I) $\pi^-p \rightarrow n^* \rightarrow n(\pi\pi)_{I=J=0}$ and (II) $\pi^-p \rightarrow n^* \rightarrow \Delta\pi \rightarrow n\pi^+\pi^-$. The (I) amplitude has a constant sign, all over the available

phase space. However, process (II) has an amplitude approximately proportional to the scalar product of the final pions momenta. Therefore, it changes sign when passing from low to high invariant masses. In fact, not only is there destructive interference at low masses, the constructive interference increases the size of the high mass region.

Our results for Calcium are shown in fig. 7. Again, there is a very good agreement with the $\pi^+\pi^+$ data. The shape of the figure is quite similar to the deuteron case. There is some softening, and the distribution reaches higher masses. Both features are mostly due to the Fermi motion of nucleons. Pion absorption is weak at low energies. Hence, it does not affect much the final pions, although it is partly responsible for the reduction of the spectral function at high masses. More important is the initial pion absorption, which apart from changing the total cross section, prevents the pions from reaching the nucleus core, therefore decreasing the effective density at which the reaction happens, and modulating all nuclear effects.

The quality of the agreement on the latter channel, gives us confidence that all standard nuclear effects are properly taken into account. In particular that we have a proper description of where in the nucleus the reaction takes place.

Finally, let us discuss the $\pi^+\pi^-$ data, the channel in which the nuclear dependent $\pi\pi$ interaction in the scalar isoscalar channel could be responsible of the presence of a low mass peak. Our results show some enhancement close to threshold, even when the pion FSI is calculated in vacuum. This is due to Fermi motion. In the full calculation, the inclusion of the medium dependence in the FSI leads to a further enhancement and a displacement towards low masses, although is not enough to reproduce the data.

One first question is the consistency of our results with those of ref. [1], which reproduce well the experiment. In order to do a proper comparison, we should impose some approximations that were used there. In particular, we find that pion absorption forces the reaction to occur at the nuclear surface, at densities lower than those used in ref. [1]. If we impose a high fixed average density (see fig. 8), we also get a large, although insufficient enhancement, and too high values for the mass distribution at high masses, produced by the

excess of Fermi motion. If we neglect pion absorption, the results follow closely the curve corresponding to $\rho = 0.5\rho_0$, as expected, given the fact that for the Calcium nucleus, the average density is approximately half the nuclear density.

In order to facilitate further the comparison with the results of ref. [1] we have also considered a simplified model for the reaction, neglecting all terms with a Δ resonance. The two curves in fig. 9 correspond to FSI calculated in vacuum and with a density $\rho = 0.5\rho_0$. This simplified model has a similar structure to that of ref. [1], and although it is able to reproduce the peaks structure in nuclei, it does so at the price of overestimating for the deuteron case the threshold region by a large factor.

VI. CONCLUSIONS

We have studied the $A(\pi^+, \pi^+\pi^\pm)X$ reactions on the deuteron and on Calcium using a realistic model for the elementary $\pi N \rightarrow \pi\pi N$ production, and including several nuclear medium effects, like Fermi motion, pion absorption, pion quasielastic scattering, and the medium dependent $\pi\pi$ interaction in the scalar isoscalar channel.

We find a very good agreement with the experimental data for the $\pi^+\pi^+$ production, which gives us confidence on our treatment of the common nuclear effects. However, we are unable to reproduce fully the strong enhancement close to the two pion threshold found in the experiment for the $\pi^+\pi^-$ production. We also find that approximations previously used in the literature could be critical in reproducing such an enhancement. Several possibilities open up. It could happen that the $\pi\pi$ interaction in the σ channel has a stronger dependence on density than that provided by existing models. This would be most interesting. However, we have also found that the smallness of the spectral function in the deuteron, close to threshold, is due to destructive interference between large pieces of the amplitude. If some of these pieces is substantially modified in the nuclear medium, the interference could disappear, and the spectral function would look more like phase space, as it is the case for $\pi^+\pi^+$ production. This would be enough to reproduce the experimental data. New dedi-

cated experiments, with a wider phase space, and at lower energies, where the interference effects are smaller are important to settle these questions.

We also find that absorption of the incoming pion, leads the reaction to occur at the surface, therefore reducing the signals of any density dependent effect. Electromagnetically induced reactions, free from such a disadvantage are clearly called for to investigate the medium effects on the $\pi\pi$ interaction in the σ channel

ACKNOWLEDGMENTS

One of us (M.J.V.V.) would like to acknowledge useful discussions with L.L. Alvarez-Ruso, N. Grion and P. Camerini. This work has been partially supported by DGYCIT contract no. PB-96-0753.

APPENDIX A: LAGRANGIANS USED IN THE $\pi N \rightarrow \pi\pi N$ MODEL

1. Pions and nucleons

The scattering amplitude of the mechanisms depicted in fig. 4, considering only nucleons for the internal lines, can be derived from the chiral lagrangians with the inclusion of baryons of ref. [16,35–37]. The relevant pieces can be written as

$$L = L_{\pi\pi} + L_{\pi N}, \quad (\text{A1})$$

In this equation, $L_{\pi\pi}$ contains the purely mesonic interaction and $L_{\pi N}$ the meson(s)-nucleon terms. The mesonic part is given by

$$L_{\pi\pi} = \frac{f^2}{4} \langle \partial_\mu U^\dagger \partial^\mu U + \chi(U + U^\dagger) \rangle, \quad (\text{A2})$$

The brackets indicate the sum in flavour space. The matrices U and u are defined by

$$U(\Phi) = u(\Phi)^2 = \exp \left\{ i\sqrt{2}\Phi/f \right\} \quad (\text{A3})$$

where

$$\Phi \equiv \frac{1}{\sqrt{2}} \vec{\tau} \vec{\phi} = \begin{pmatrix} \frac{1}{\sqrt{2}} \pi^0 & \pi^+ \\ \pi^- & -\frac{1}{\sqrt{2}} \pi^0 \end{pmatrix}, \quad (\text{A4})$$

where $\vec{\tau}$ are the Pauli matrices and the π are the pion fields. At lowest order, f is equal to the pion decay constant, $f = f_\pi = 92.4 \text{ MeV}$. Assuming isospin symmetry, the mesonic mass matrix is

$$\chi = \begin{pmatrix} m_\pi^2 & 0 \\ 0 & m_\pi^2 \end{pmatrix}, \quad (\text{A5})$$

The interaction with the nucleon is described by the term

$$L_{\pi N} = \bar{\Psi} (i \gamma^\mu \nabla_\mu - M + \frac{g_A}{2} \gamma^\mu \gamma_5 u_\mu) \Psi. \quad (\text{A6})$$

Here, M is the nucleon mass, Ψ is the nucleon isospinor

$$\Psi = \begin{pmatrix} p \\ n \end{pmatrix}, \quad (\text{A7})$$

and $g_A \approx 1.26$ is related to the pion nucleon coupling constant ($f_{NN\pi}/m_\pi$) by the Goldberger-Treiman relation $\frac{f_{NN\pi}}{m_\pi} = \frac{g_A}{2f}$. The covariant derivative of the nucleon field $\nabla_\mu \Psi$ is given by

$$\nabla_\mu \Psi = \partial_\mu \Psi + \Gamma_\mu \Psi, \quad \Gamma_\mu = \frac{1}{2} (u^\dagger \partial_\mu u + u \partial_\mu u^\dagger). \quad (\text{A8})$$

Expanding U and u , and keeping the terms with up to four pion fields, the following set of Lagrangians are obtained,

$$L_{\pi\pi\pi\pi} = \frac{1}{6f_\pi^2} \left[(\partial_\mu \vec{\phi})^2 - \vec{\phi}^2 (\partial_\mu \vec{\phi})^2 + \frac{1}{4} m_\pi^2 \vec{\phi}^4 \right], \quad (\text{A9})$$

$$L_{NN\pi} = -\frac{f_{NN\pi}}{m_\pi} \bar{\Psi} \gamma^\mu \gamma_5 \partial_\mu \vec{\phi} \vec{\tau} \Psi, \quad (\text{A10})$$

$$L_{NN\pi\pi\pi} = \frac{1}{6f_\pi^2} \frac{f_{NN\pi}}{m_\pi} \bar{\Psi} \gamma^\mu \gamma_5 [(\partial_\mu \vec{\phi} \vec{\tau}) \vec{\phi}^2 - (\vec{\phi} \vec{\tau}) (\partial_\mu \vec{\phi} \vec{\phi})] \Psi, \quad (\text{A11})$$

$$L_{NN\pi\pi\pi} = -\frac{1}{4f_\pi^2} \bar{\Psi} \gamma^\mu \vec{\tau} (\vec{\phi} \times \partial_\mu \vec{\phi}) \Psi. \quad (\text{A12})$$

Whereas the expression of the $L_{NN\pi}$ Lagrangian is quite standard, different forms can be found in the literature for the A9 and A11 pieces, because different representations for the pion field $U(\Phi)$ had been used. However, it can be shown that they produce the same physical amplitudes. In particular, they are equivalent to the Weinberg Lagrangians used in ref. [20] when the chiral symmetry breaking parameter ξ is taken to be zero.

The $L_{NN\pi\pi}$ term describes the isovector part of the $\pi N \rightarrow \pi N$ s-wave interaction. The very small isoscalar part would appear at higher orders of the chiral Lagrangian. Adding a phenomenological isoscalar part, and doing a low energy approximation, the Lagrangian can be recast in the typical form

$$L_{NN\pi\pi} = -4\pi \left\{ \frac{\lambda_1}{m_\pi} \bar{\Psi} \vec{\phi}^2 \Psi + \frac{\lambda_2}{m_\pi^2} \bar{\Psi} \vec{\tau} (\vec{\phi} \times \partial_t \vec{\phi}) \Psi \right\}. \quad (\text{A13})$$

where $\lambda_2 = \frac{m_\pi^2}{16\pi f_\pi^2} \approx 0.045$. Fitting the constants to the s-wave πN scattering lengths [38], one gets an slightly larger $\lambda_2 = 0.52$, and $\lambda_1 = 0.048$.

Finally, the pion and nucleon propagators are

$$D_\pi(q) = \frac{1}{q^2 - m_\pi^2}, \quad (\text{A14})$$

$$G_N(q) = \frac{M}{E_q} \frac{1}{q^0 - E_q + i\epsilon}, \quad (\text{A15})$$

where $E_q = \sqrt{q^2 + M^2}$

2. Δ resonance

Diagrams d) and e) of fig. 4 could also have Δ resonances as intermediate steps. The required $\Delta N\pi$ and $\Delta\Delta\pi$ vertices are described by the following phenomenological Lagrangians

$$L_{\Delta N\pi} = \frac{f^*}{m_\pi} \psi_\Delta^\dagger S_i^\dagger (\partial_i \vec{\phi}) \mathbf{T}^\dagger \psi_N + h.c., \quad (\text{A16})$$

$$L_{\Delta\Delta\pi} = \frac{f_\Delta}{m_\pi} \psi_\Delta^\dagger S_{\Delta i} (\partial_i \vec{\phi}) \mathbf{T}_\Delta \psi_\Delta, \quad (\text{A17})$$

where the $\psi_{\Delta(N)}^\dagger$ are two-component spinor fields, \mathbf{S}^\dagger (\mathbf{T}^\dagger), and $S_\Delta(T_\Delta)$ are the spin (isospin) $1/2 \rightarrow 3/2$ and $3/2 \rightarrow 3/2$ transition operators. Definition, and some useful algebraic relations of this operators can be found in ref. [39].

The Δ propagator is given by

$$G_\Delta(p) = \frac{1}{W - M_\Delta + \frac{1}{2}i\Gamma_\Delta(p)} \quad (\text{A18})$$

where W is the Δ invariant mass and the resonance width Γ_Δ is

$$\Gamma_\Delta(W) = \frac{1}{6\pi} \left(\frac{f^*}{m_\pi} \right)^2 \frac{M}{W} |\mathbf{q}_{\text{cm}}|^3 \Theta(W - M - m_\pi). \quad (\text{A19})$$

with \mathbf{q}_{cm} the pion momentum in the resonance rest frame. The $\Delta N\pi$ coupling constant, obtained from πN phase shifts or from the experimental width, using eq. A19, takes the value $f^* = 2.13$. For the $\Delta\Delta\pi$ coupling we take the quark model value, $f_\Delta = 4/5 f_{N\pi}$ [40].

3. Roper resonance

The Roper resonance can decay into a nucleon and a pion, a Δ and a pion and a nucleon and two s-wave pion. The effective Lagrangians we use to describe these interactions are

$$L_{N^*N\pi} = -\frac{\tilde{f}}{m_\pi} \bar{\Psi}_{N^*} \gamma^\mu \gamma_5 \partial_\mu \vec{\phi} \vec{\tau} \Psi_N + h.c., \quad (\text{A20})$$

$$L_{N^*\Delta\pi} = \frac{f_{N^*\Delta\pi}}{m_\pi} \psi_\Delta^\dagger S_i^\dagger (\partial_i \vec{\phi}) \mathbf{T}^\dagger \psi_{N^*} + h.c.. \quad (\text{A21})$$

and

$$L_{N^*N\pi\pi} = -C \bar{\Psi}_{N^*} \vec{\phi} \vec{\phi} \Psi_N + h.c.. \quad (\text{A22})$$

The coupling constants \tilde{f} , $f_{N^*\Delta\pi}$ and C are calculated from the N^* width and branching ratios. There are considerable uncertainties in the experimental information, but using the central values from ref. [41] one gets $\tilde{f} = 0.477$, $f_{N^*\Delta\pi} = 2.07$ and $C = 2.3m_\pi^{-1}$ [39]. The Roper propagator is given by

$$G_{N^*}(p) = \frac{1}{W - M^* + \frac{1}{2}i\Gamma_{N^*}(p)} \quad (\text{A23})$$

At low energy, the width is dominated by the decay into the $N\pi$ channel, and it is given by

$$\Gamma_{N^*} \approx \Gamma_{N\pi} = \frac{3}{2\pi} \left(\frac{\tilde{f}}{m_\pi} \right)^2 \frac{M}{W} |\mathbf{q}_{\text{cm}}|^3 \Theta(W - M - m_\pi). \quad (\text{A24})$$

Whereas all other constants are obtained from different experiments, without two s-wave pions in the final state, and hence are independently determined, we should handle with more care $f_{N^*\Delta\pi}$ and C . Both constants correspond to processes with two pions in the final state, which could be in the scalar isoscalar channel. The constants have been fitted to the experimental Roper partial widths using the Born approximation (without final state interaction of the pions), and therefore effectively incorporate already the vacuum renormalization due to the final state interaction of the pions. As we will include the FSI explicitly in our calculation, we have first to discount its effects on these two constants to avoid double counting.

As explained in Sec. III A our model implements FSI by multiplying the scalar isoscalar part of the amplitude by the factor \mathcal{F} . This factor depends smoothly in vacuum on the invariant mass of the two pion system, and is practically constant over the available phase space region of the $N^*(1440)$ decay. We thus take a corrected value for C

$$C \rightarrow \frac{C}{|\bar{\mathcal{F}}|}, \quad (\text{A25})$$

where $\bar{\mathcal{F}}$ is the value of \mathcal{F} at the average invariant mass of the two pions in the $N^*(1440)$ decay. The correction is not as important for the $f_{N^*\rightarrow\Delta\pi}$ case. First, because only a small part of the partial width produces pion pairs in the scalar isoscalar channel, and second because at the low energies of the experiment under analysis, the contribution of this kind of mechanisms is small.

REFERENCES

- [1] R. Rapp *et al.*, Phys. Rev. **C59**, R1237 (1999).
- [2] T. Hatsuda, T. Kunihiro and H. Shimizu, Phys. Rev. Lett. **82**, 2840 (1999); T. Hatsuda, T. Kunihiro, H. Shimizu, nucl-th/9810022; T. Kunihiro, hep-ph/9905262.
- [3] F. Bonutti *et al.*, Phys. Rev. Lett. **77**, 603 (1996).
- [4] F. Bonutti *et al.*, Nucl. Phys. **A638**, 729 (1998).
- [5] G. Janssen, B.C. Pearce, K. Holinde and J. Speth, Phys. Rev. **D52**, 2690 (1994); D. Lohse, J.W. Durso, K. Holinde and J. Speth, Nucl. Phys. **A516**, 513 (1990).
- [6] J.A. Oller, E. Oset, Nucl. Phys. **A620**, 438 (1997); J.A. Oller, E. Oset and J.R. Pelaez, Phys. Rev. Lett. **80**, 2452 (1998).
- [7] P. Schuck, W. Nörenberg and G. Chanfray, Z. Phys. **A330**, 119 (1988).
- [8] G. Chanfray, Z. Aouissat, P. Schuck and W. Nörenberg, Phys. Lett. **B256**, 325 (1991);
- [9] V. Mull, J. Wambach and J. Speth, Phys. Lett. **B286**, 13 (1992).
- [10] Z. Aouissat, G. Chanfray and P. Schuck, Mod. Phys. Lett. **A15**, 1379 (1993).
- [11] R. Rapp, J.W. Durso and J. Wambach, Nucl. Phys. **A596**, 436 (1996).
- [12] Z. Aouissat, R. Rapp, G. Chanfray, P. Schuck, and J. Wambach, Nucl. Phys. **A581**, 471 (1995).
- [13] H.C. Chiang, E. Oset and M.J. Vicente-Vacas, Nucl. Phys. **A644**, 77 (1997).
- [14] P. Camerini *et al.*, Nucl. Phys. **A552**, 451 (1993).
- [15] F. Bonutti *et al.*, Phys. Rev. C (1999)
- [16] J. Gasser and H. Leutwyler, Nucl. Phys. **B 250**, 465 (1985).
- [17] G. Chanfray and D. Davesne, Nucl. Phys. **A 646**, 125 (1999).

- [18] E. Oset, H. Toki, W. Weise, Phys. Rept. **83**, 281 (1982).
- [19] P. Schuck *et al.*,nucl-th/9806069.
- [20] E. Oset, M.J. Vicente Vacas, Nuc. Phys.**A 446**, 584 (1985).
- [21] O. Jaekel, M. Dillig, C. A. Z. Vasconcelos, Nucl. Phys. **A541**, 673 (1992).
- [22] V. Bernard, N. Kaiser and U.G. Meissner, Nucl. Phys. **B457**, 147 (1995); *ibid.* **A 619**, 261 (1997).
- [23] T.S. Jensen and A.F. Miranda, Phys. Rev. **C55**, 1039 (1997).
- [24] A.A. Bolokhov, M.V. Polyakov and S.G. Sherman, Eur. Phys. J. **A1**, 317 (1997).
- [25] V. Sossi *et al.*, Nucl. Phys. **A 548**, 562 (1992).
- [26] G. Kernel *et al.*, Phys. Lett. **B216**, 244 (1989).
- [27] C.W. Bjork *et al.*, Phys. Rev. Lett. **44**, 62 (1980).
- [28] J. Lowe *et al.*, Phys. Rev. **C44**, 956 (1991).
- [29] A.A. Belkov *et al.*, Sov. J. Nucl. Phys. **31**, 96 (1980).
- [30] S.A. Bunyatov *et al.*, Sov. J. Nucl. Phys. **25**, 177 (1977).
- [31] M.E. Sevier *et al.*, Phys. Rev. Lett. **66**, 2569 (1991).
- [32] G. Kernel *et al.*, Z. Phys. **C48**, 201 (1990).
- [33] E. Oset, M.J. Vicente Vacas, Nucl. Phys. **A 454**, 637 (1986).
- [34] C.W. De Jager, H. De Vries and C. De Vries, Atom. Data Nucl. Data Tabl. **14**, 479 (1974).
- [35] U.G. Meissner, Rep. Prog. Phys. **56**, 903 (1993); V. Bernard, N. Kaiser and U.G. Meissner, Int. J. Mod. Phys. **E 4**, 193 (1995).

- [36] A. Pich, Rep. Prog. Phys. **58**, 563 (1995).
- [37] G. Ecker, Prog. Part. Nucl. Phys. **35**, 1 (1995).
- [38] R. Koch, Nucl. Phys. **A448**, 707 (1986).
- [39] L. Alvarez-Ruso, E. Oset and E. Hernandez, Nucl. Phys. **A633**, 519 (1998).
- [40] G.E. Brown and W. Weise, Phys. Rept. **22**, 279 (1975).
- [41] C. Caso *et al.*, Eur. Phys. J. **C3**, 1 (1998).

FIGURES

FIG. 1. Diagrammatic representation of the Bethe-Salpeter equation.

FIG. 2. Some new terms of the Bethe-Salpeter equation in nuclear matter. Bubbles represent particle-hole and Δ -hole excitations.

FIG. 3. $\text{Im } T_{\pi\pi}$ in the scalar isoscalar channel at different nuclear densities as a function of the CM energy of the pion pairs. The labels correspond to the nucleons Fermi momentum.

FIG. 4. Feynman diagrams contributing to the $\pi N \rightarrow \pi\pi N$ reaction. Dashed lines are pions. External solid lines are nucleons. Internal solid lines are nucleons, Δ 's and $N^*(1440)$ where possible.

FIG. 5. Total cross section for the $\pi N \rightarrow \pi\pi N$ reaction vs. pion kinetic energy. Upper box: $\pi^- p \rightarrow \pi^+ \pi^- n$; Experimental points from refs. [26,27]. Middle box: $\pi^- p \rightarrow \pi^0 \pi^0 n$; Data from refs. [28–30]. Lower box: $\pi^+ p \rightarrow \pi^+ \pi^+ n$; Data from refs. [31,32].

FIG. 6. Two pion invariant mass distributions in the $\pi^- + d \rightarrow \pi^+ \pi^- nn$ (upper box), and $\pi^+ + d \rightarrow \pi^+ \pi^+$ (lower box) reactions. Experimental points are from ref. [15].

FIG. 7. Two pion invariant mass distributions in the $\pi^- + Ca \rightarrow \pi^+ \pi^- X$ (upper box), and $\pi^+ + Ca \rightarrow \pi^+ \pi^+ X$ (lower box) reactions. Solid line, full calculation; dashed line, no medium effects in the FSI of the two pions. Experimental points are from ref. [3].

FIG. 8. Same as fig. 7, using a fixed averaged density. Short dashed line, $\rho = 0.5\rho_0$; long dashed line $\rho = 0.7\rho_0$. Solid line, full calculation

FIG. 9. Same as fig. 7, using a fixed averaged density $\rho = 0.7\rho_0$ and a simplified model (see text). Dashed line, FSI in vacuum; Solid line, FSI in medium.

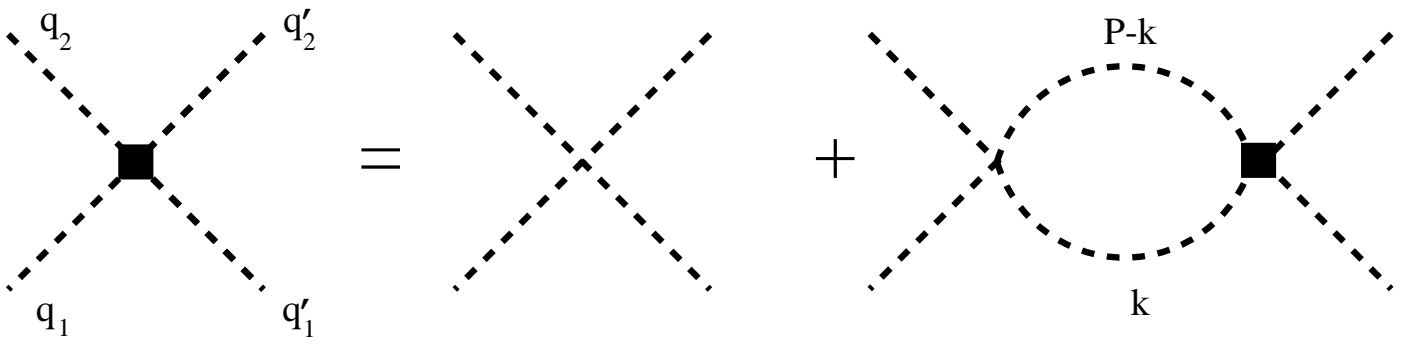


Figure 1

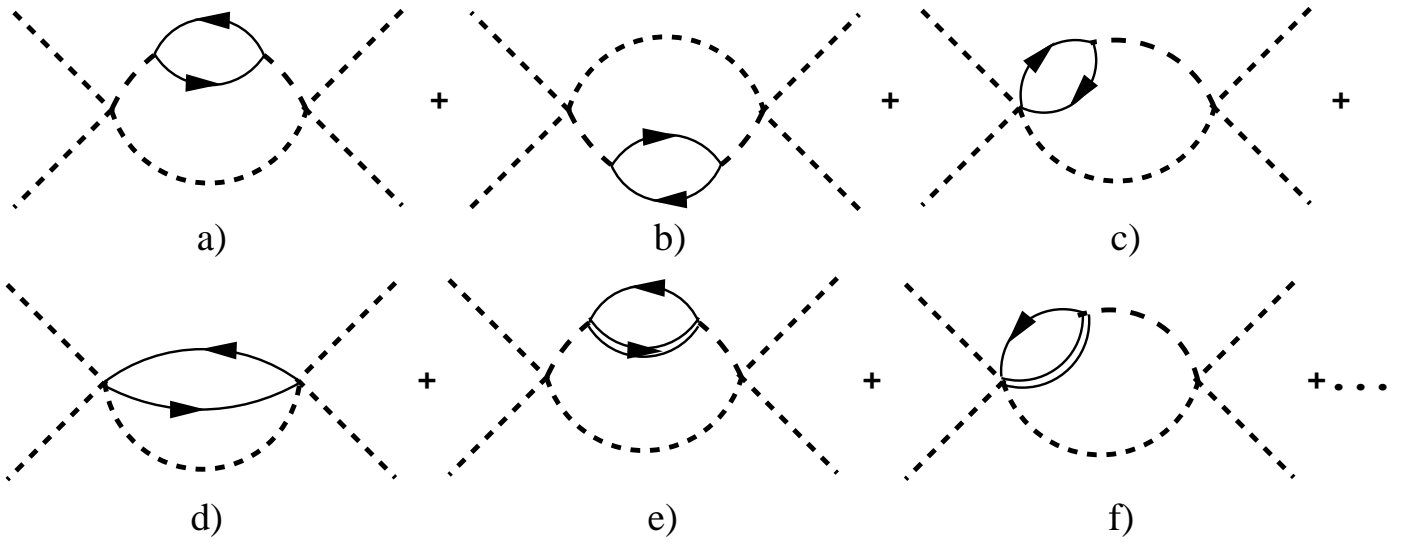


Figure 2

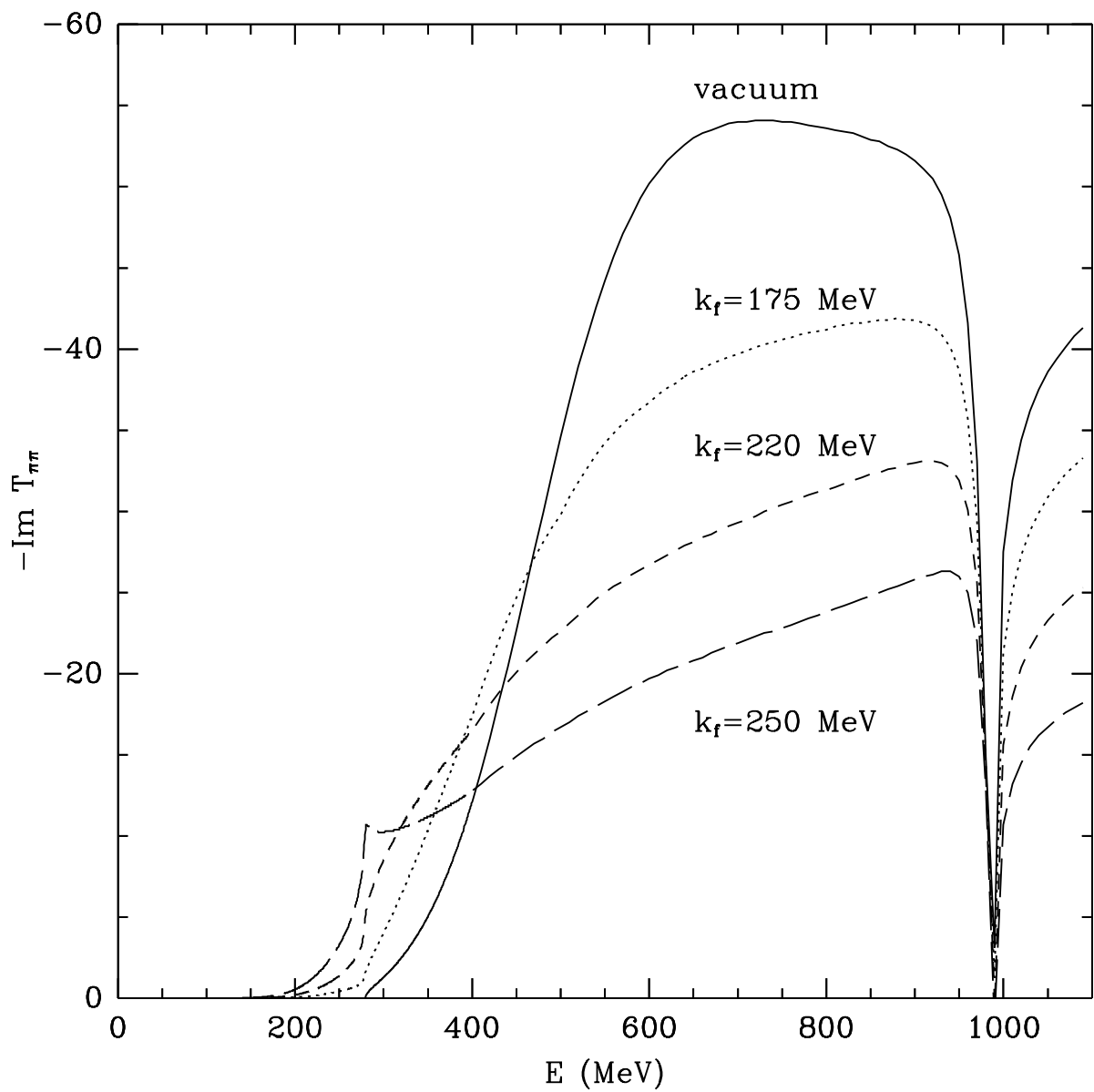


Figure 3

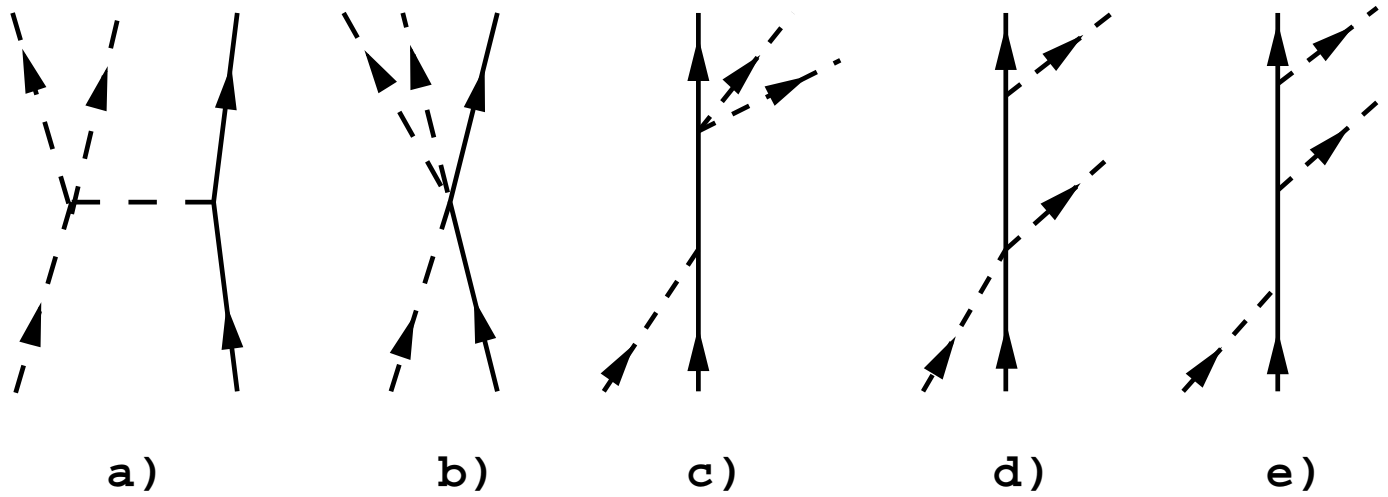


Figure 4

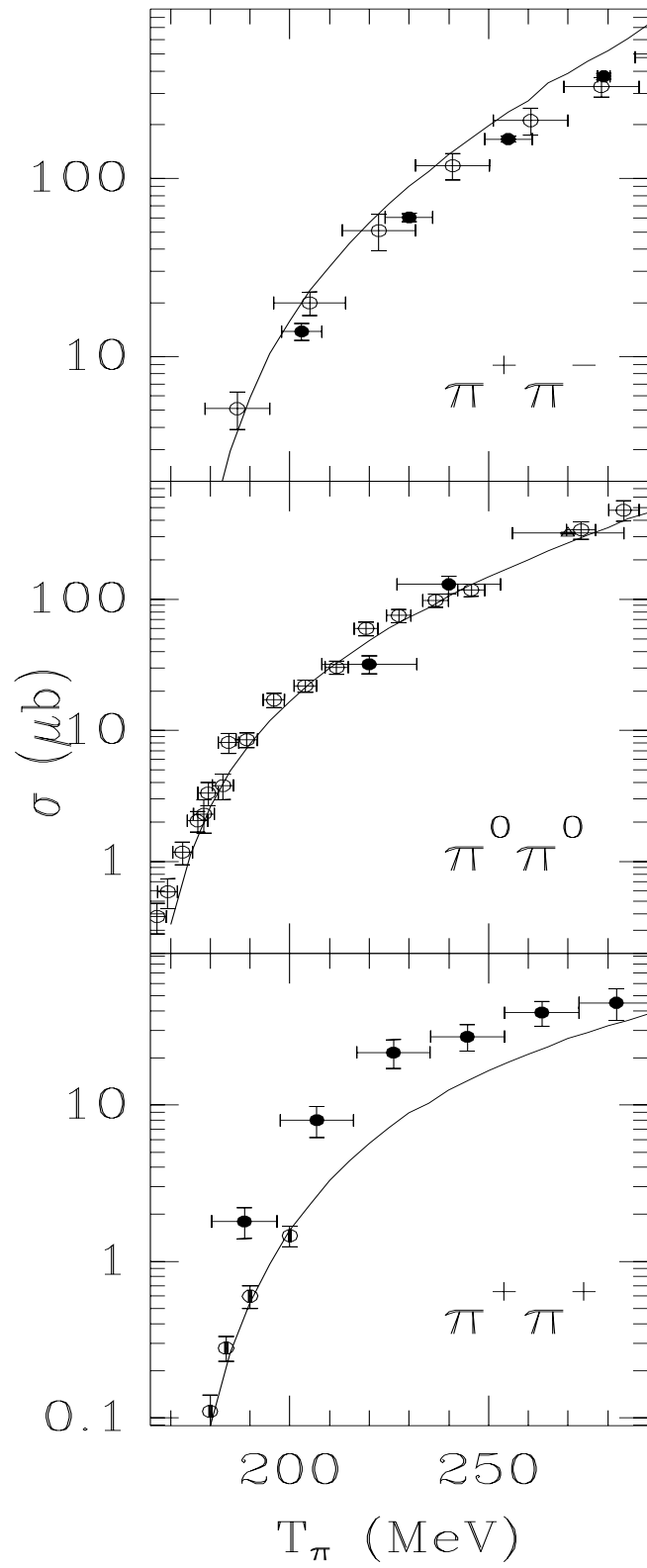


Figure 5

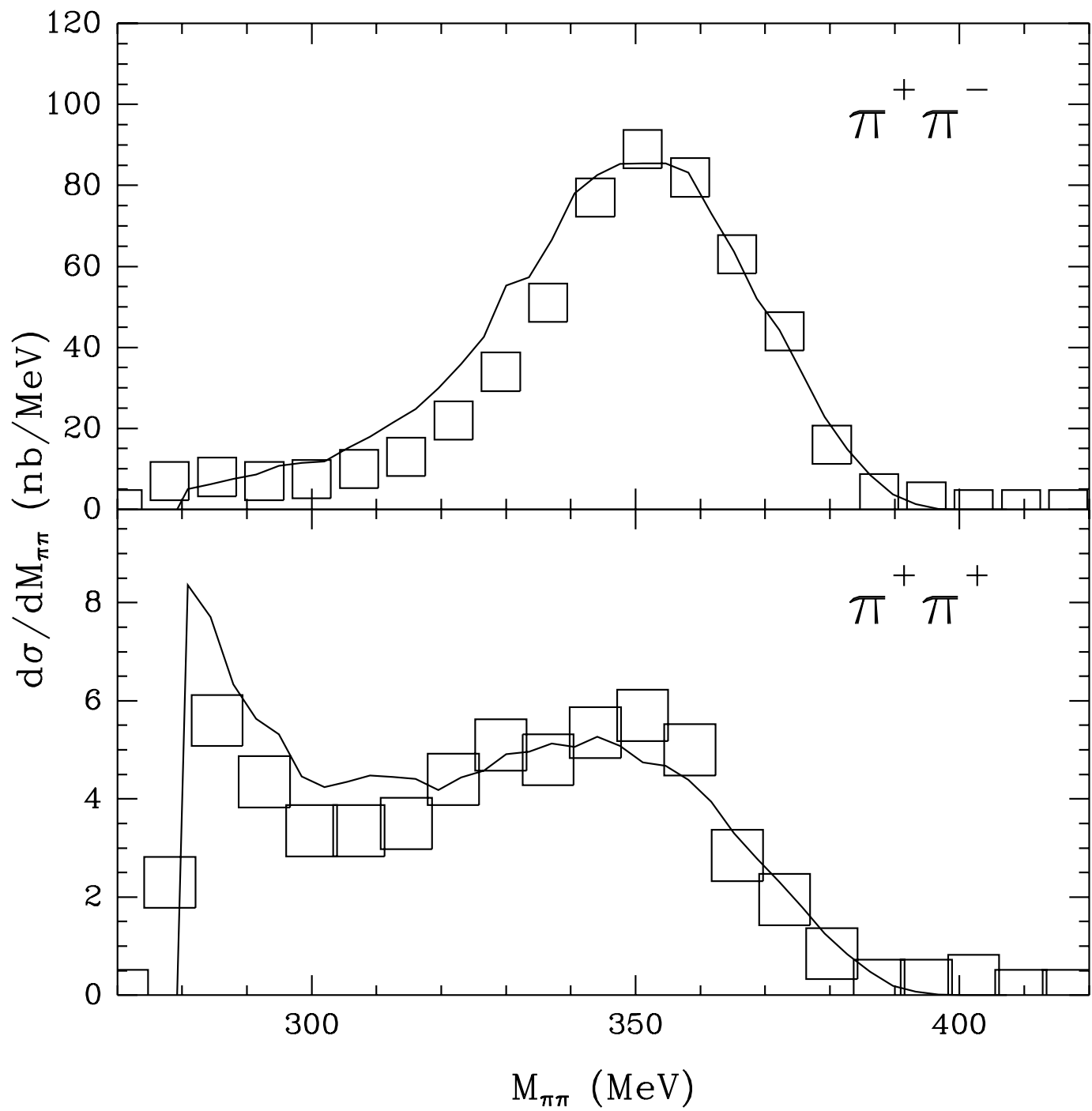


Figure 6

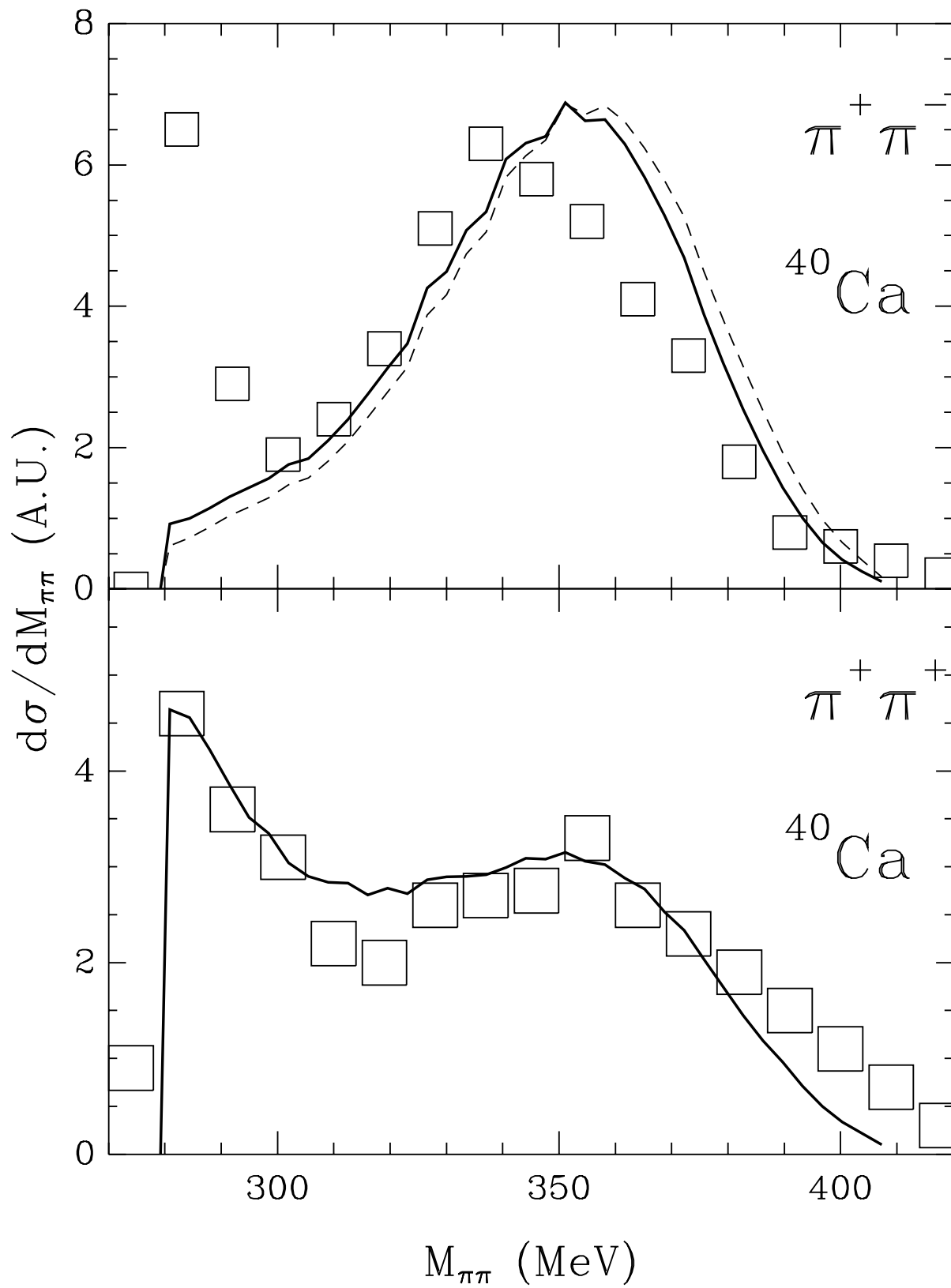


Figure 7

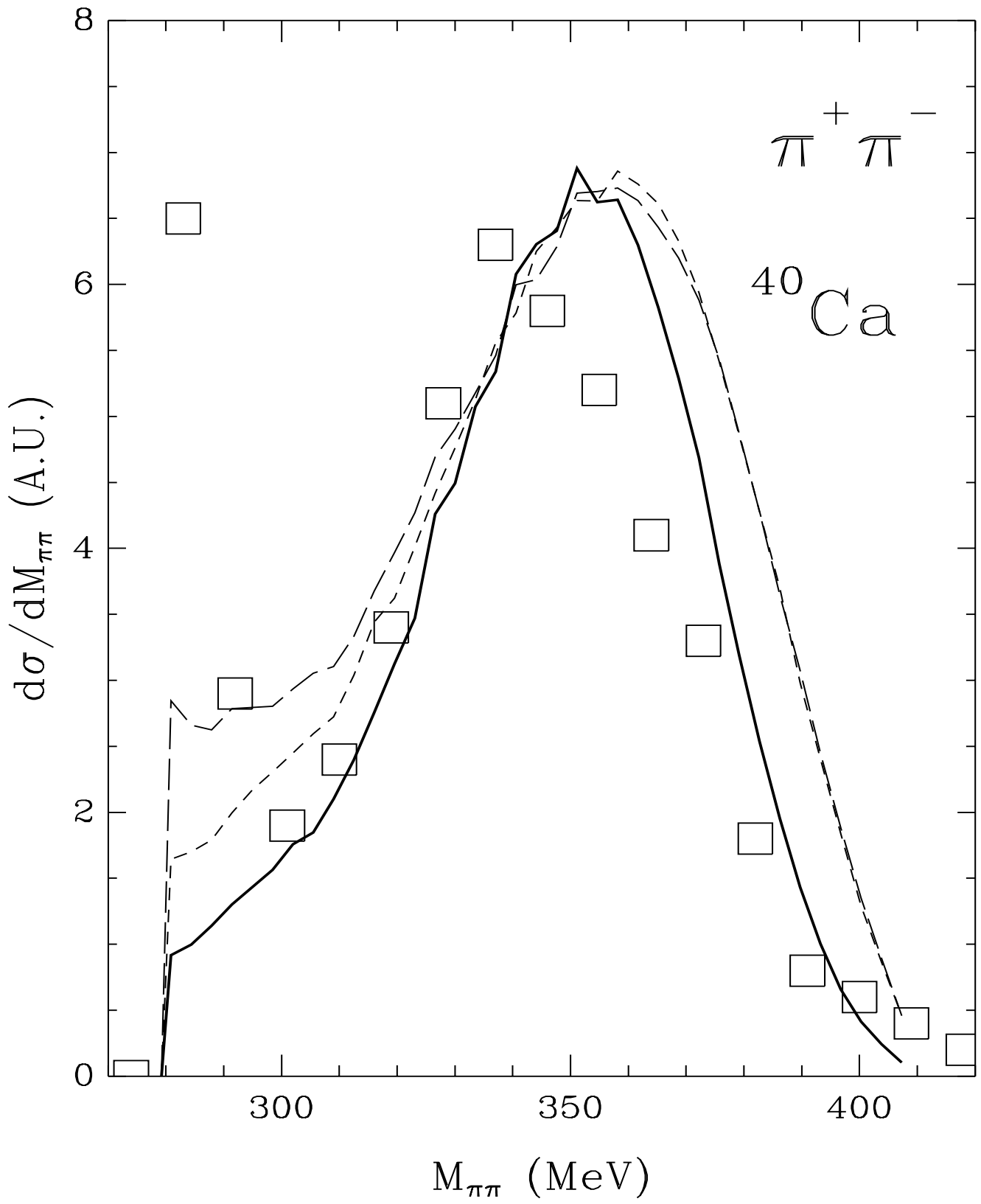


Figure 8

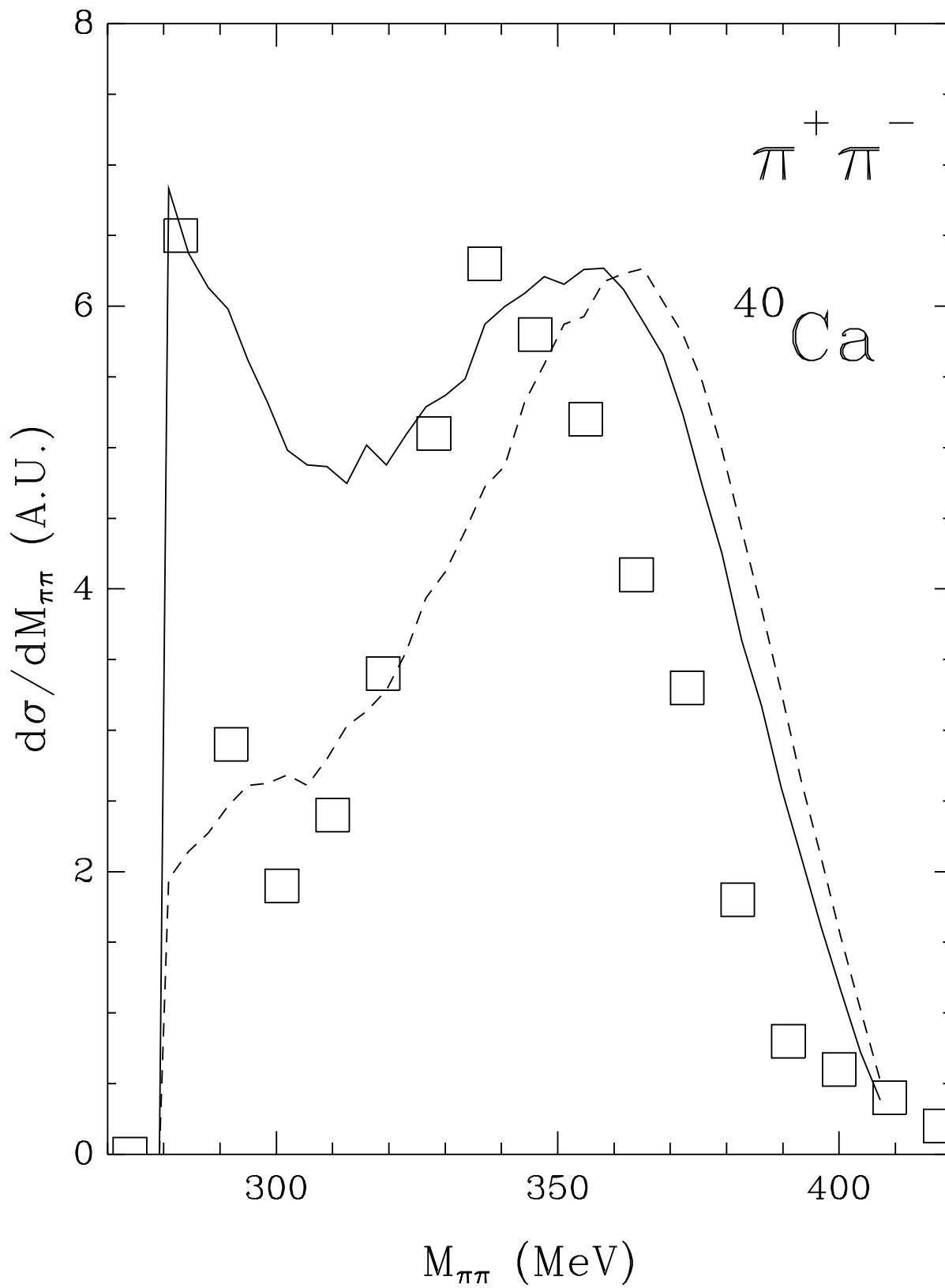


Figure 9